A fast method for estimation of light flux in fluorescence image guided surgery

1. Introduction

In this document, we present a theoretical method to estimate the light flux in near-infrared fluorescence imaging of tissues. This technique can potentially be used in the clinic to detect and locate, in real time, structures such as lymph nodes or appropriately labelled tumour tissue located at depths of a few millimetres (and up to 15-20 mm) below the tissue surface. The modelling software described here has been implemented to allow the user to set pertinent parameters such as tissue and dye properties, imaging optics, excitation characteristics and system geometry. While not as accurate as established models [1], our approach has the advantage of *speed of execution*, allowing the user to 'try out' a variety of experimental conditions. Moreover, it covers the whole photon 'journey', from excitation to image visualization. The software can be downloaded as a standalone executable for Microsoft Windows platforms from our website.

This work addresses the commonly asked questions: "What is the sensitivity, how many molecules will I be able to detect? What is the spatial resolution?" etc. Of course every case is different (e.g. excitation and emission wavelengths) but a simple method to relate known physical parameters (such as dye and detector quantum efficiencies, light source excitation power, collection efficiency) and biologically relevant parameters (dye concentration, number of molecules in the sample etc.) to derive an expected image was thought to be useful. There will always be a trade off between imaging depth and image quality but in fluorescence image-guided surgery what is often required is the ability to see 'something' in real time, without complex on-line image processing. The approach presented here aims to address this, and the software application is intended to give approximate answers and to indicate the limits of what can be detected with a given fluorescence imaging system applied to imaging at depth.

We have applied this model to estimate the detection limits of widefield and laparoscopic fluorescence imaging systems operating in the near infrared portion of the electromagnetic spectrum, using semiconductor lasers as sources of excitation light and sensitive CCD or EMCCD imaging detectors, operating at video rates (20 ms integration) and at longer, but still short, integration times (40 ms - ~1 sec).

2. Tissue optics

Light propagation in biological tissues is characterised by interactions with numerous components, ranging from ions and small molecules like water or sugars, to larger structures such as cells. When an interaction occurs, a photon can be either absorbed, or transmitted or scattered. As we move towards the infrared region of the optical spectrum, the probability of light absorption by oxyhaemoglobin and deoxyhaemoglobin decreases. On the other hand, the absorption by water molecules increases and becomes dominant, reaching a peak at ~950 nm. This results in an optimal spectral region (also known as near infrared (NIR) window (650-900 nm)) where the average photon penetration depth is of the order of 10 mm.

A scattering event occurs when the photon is deflected from its original trajectory. The average deflection angle depends mostly on the characteristics of the medium. In biological tissues, the anisotropy factor g is usually close to 1, meaning that the photon is likely to be deflected through small angles (<10 degrees). In the NIR region, scattering dominates over absorption, making it the principle mechanism associated with light propagation. As a result, a photon undergoes a high number of scattering events, losing track of its original direction. This means that, despite the small average deflection angles, at depths > 1-2 mm the photon's direction can be considered randomised.

The Monte Carlo technique [2] provides the most accurate tool to model light transport in tissue, particularly under the above conditions. Because of its ability to simulate every interaction event, this method is considered the gold standard in tissue optics. However, when the performance is

related to computation time, Monte Carlo might not be optimal, especially if we are not interested in achieving high accuracy. For this reason, we developed an analytical model that uses light transport equations and adjusts them according to the more accurate Monte Carlo process.

3. The model geometry

The model is designed to simulate practical situations where a portion of tissue is excited with light at a given wavelength (in our case 785 nm) and an imaging system collects fluorescence light from a specific field of view. A fluorophore (sample) is located on the surface or at some depth in tissue. The dimensions of the sample are considered to be much smaller than the field of view. The dimensions of the sample are such that, had it been present on the surface of the sample, it would have been imaged with a single imager pixel. This choice was made in order to emphasize the loss of resolution as the sample is moved deeper. In order to simplify the problem, we consider the excitation power density to be homogeneous on the tissue surface. We also assume that the medium that contains the fluorescent sample has uniform absorption and scattering characteristics, both for excitation and fluorescence emission light.
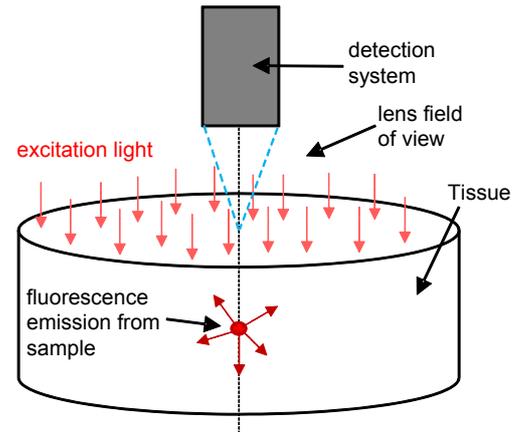

Figure 1: Geometry of the system: the excitation light power density has been considered homogeneous on the tissue surface.

4. Excitation

We performed Monte Carlo simulations using the code developed by Prahl et al. [2]. The code was slightly modified and adjusted to our particular situation. A high number of photons (10^7) were launched and the average photon density at different depths was scored, as shown in Figure 2(a). As the excitation beam is large compared to the fluorescent target, the photon fluence rate decays exponentially following the Beer-Lambert law [3]. A comparison of the results is shown in Figure 2(b). If we consider that the computation time for the Monte Carlo simulation was ~3.5 hours (using an Intel 2 Core processor, 4 GB memory), the analytical model proved to be significantly more efficient, taking ~16 ms to compute the results. Several tests were made changing tissue parameters and the same level of accuracy was obtained.
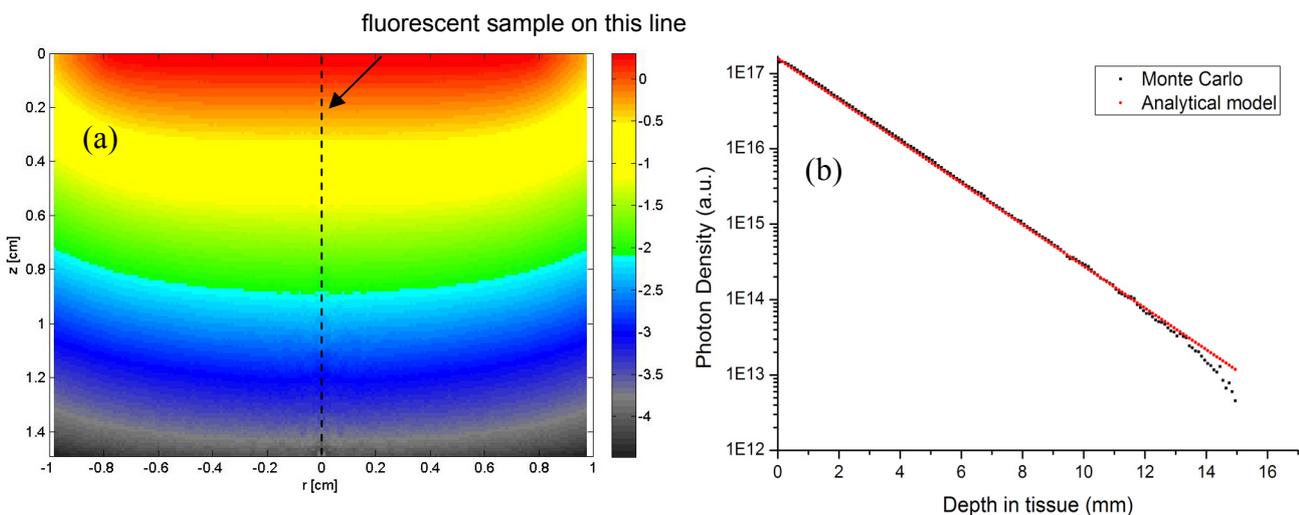

Figure 2: (a) Logarithmic scale false colourmap of photon density of an 8 mm radius excitation beam determined by Monte Carlo simulation. The dotted line indicates that the target sample is located at the centre of the excitation beam. (b) The photon density values at the beam centre agree with the results from the analytical model. (Light wavelength = 785 nm, absorption coefficient μ_A = 0.38 cm^{-1}, scattering coefficient μ_S = 350 cm^{-1}, anisotropy factor g = 0.9, refractive index n = 1.33).

When a photon interacts with a molecule of the dye, the target has an average probability (cross section σ) to absorb the incoming photon. This probability depends on the dye and on the wavelength of the excitation light, and for most fluorophores the cross section is of the order of 10^{-16} cm^2 per molecule [4]. This is the value that has been assumed here.

5. Emission

When a molecule absorbs a photon, its energy level is increased, causing the molecule to jump to an excited singlet state. The emission process takes place when most of the energy gained through absorption is released; in the case of luminescent molecules, this energy release generates light at a higher wavelength (lower energy). The conversion rate is expressed by the quantum yield (*QY*) which, for many organic near NIR dyes is of the order of 1-5 %. If the incident light flux (photons/sec/cm^2) is *I*, the fluorescence produced *F* (photons/sec) by a single molecule of fluorophore is expressed by the equation:

$$F = I \times QY \times \sigma$$

where σ is the molecular absorption cross-section. Since fluorescence emission is an isotropic process, the situation becomes more complex compared to excitation. We modified the Monte Carlo code from [2], designed only for transport of a pencil beam of light, and adjusted it for the geometry of the emission process. A photon is launched from the position of the dye in the tissue and its direction is randomized over the full sphere solid angle. This is accomplished by calling the random number generator function every time an individual photon is launched; this determines its initial direction. The scored photon fluence rate is shown in Figure 3(a).
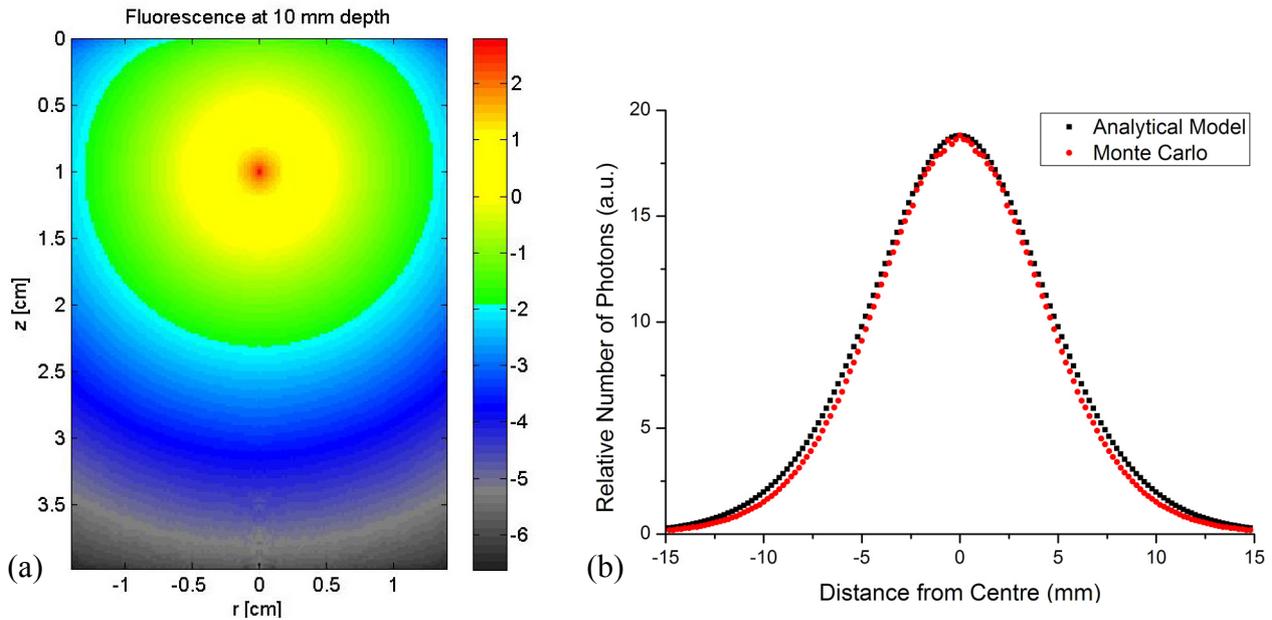

Figure 3: (a) Monte Carlo simulation of isotropic emission from a point source at 10 mm depth. Number of photons launched: 10^7, computation time: 23.63 hours, light wavelength = 785 nm, absorption coefficient $\mu_A = 0.25$ cm^{-1}, scattering coefficient $\mu_S = 280$ cm^{-1}, anisotropy factor $g = 0.9$, refractive index $n = 1.33$. (b) Photon distribution on the tissue surface compared with the analytical model. When the diffusion approximation is valid, the model agrees with the simulation, without the need of correction factors. Other tests with different parameters were performed, with similar results.

The Monte Carlo technique is of course very time consuming when the emission process is simulated. As we are only interested in the photons coming out of the tissue surface, our idea was to use photon transport equations to estimate the amount of light reaching the surface. We divided the tissue surface in small squares, each corresponding to an imaged camera pixel. We then calculated

analytically the number of dye-emitted photons that reach a specific 'pixel' on the surface. The size of the surface 'pixel' depends on the working distance of the imager and on the focal length of the optical system (in our case 25 mm). The photon distribution obtained is symmetric and centred in the origin, with a linear profile that can be approximated by a Gaussian function. The extend of the Gaussian changes with depth, indicating that deep samples will be imaged across more pixels (i.e. image blurring increases with sample depth) and that the peak intensity reduces with depth, potentially reducing contrast for non-zero backgrounds at the tissue surface. In other words, as the imaging depth increases, the resolution gets lower.

Despite its qualitative agreement with the Monte Carlo model (Figure 3(b)), the absolute number of photons in the analytical model needed a correction factor, particularly when absorption dominates over scattering. This factor and its variation with depth are provided by the Monte Carlo simulation. However, when $\mu_A << \mu_S$, which is usually the case in biological tissues, the transport equation can be approximated using the diffusion theory [5]. As a result, an excellent estimation of the photon distribution can be obtained more rapidly without the need of performing time-consuming simulations.

6. Light collection

Of course not every photon which reaches the tissue surface will be collected by the imaging system. Depending on the working distance and on the f-number of the imaging lens, only photons emerging within a given angle relative to the normal of the surface are collected. As the multiple-scattering process dominates, it is reasonable to assume that photons leave the tissue surface isotropically. However, if we score the angular distribution on the surface with the Monte Carlo method, we observe that the probability of emerging at high angle relative to the normal is reduced, as shown in Figure 4.
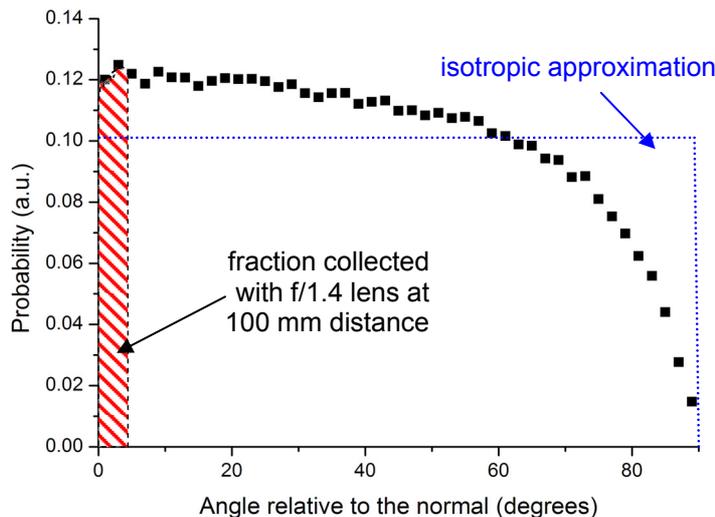

Figure 4: Angular distribution of photons coming out the tissue surface. Monte Carlo simulation was performed with the parameters described in the previous figure. The graph also shows (in blue) what an isotropic distribution would look like.

The imaging lens collection capability was calculated by integrating from zero (i.e. normal to the tissue) to the angle determined by the lens f-number and the working distance in the curve shown in Figure 4. We demonstrated that, when scattering is dominant, the shape of this curve is only marginally affected by changes in source depth and tissue parameters. As a consequence, it is reasonable to assume that the angular distribution stays the same, with no need to score it in every Monte Carlo simulation. As shown in Figure 4, the isotropic approximation for the photons emerging the tissue surface is likely to underestimate by about 20% the more accurate value. Potential light losses in the lens system are also considered.

7. FIFAC software

A software tool named FIFAC: **F**luorescence **I**maging **F**ast **A**nalytic **C**alculator was developed, using Python programming language, and aims to simplify the calculatons presented in the modelling approximation. The software flowchart is represented in Figure 5, while Figure 6 shows the software interface.
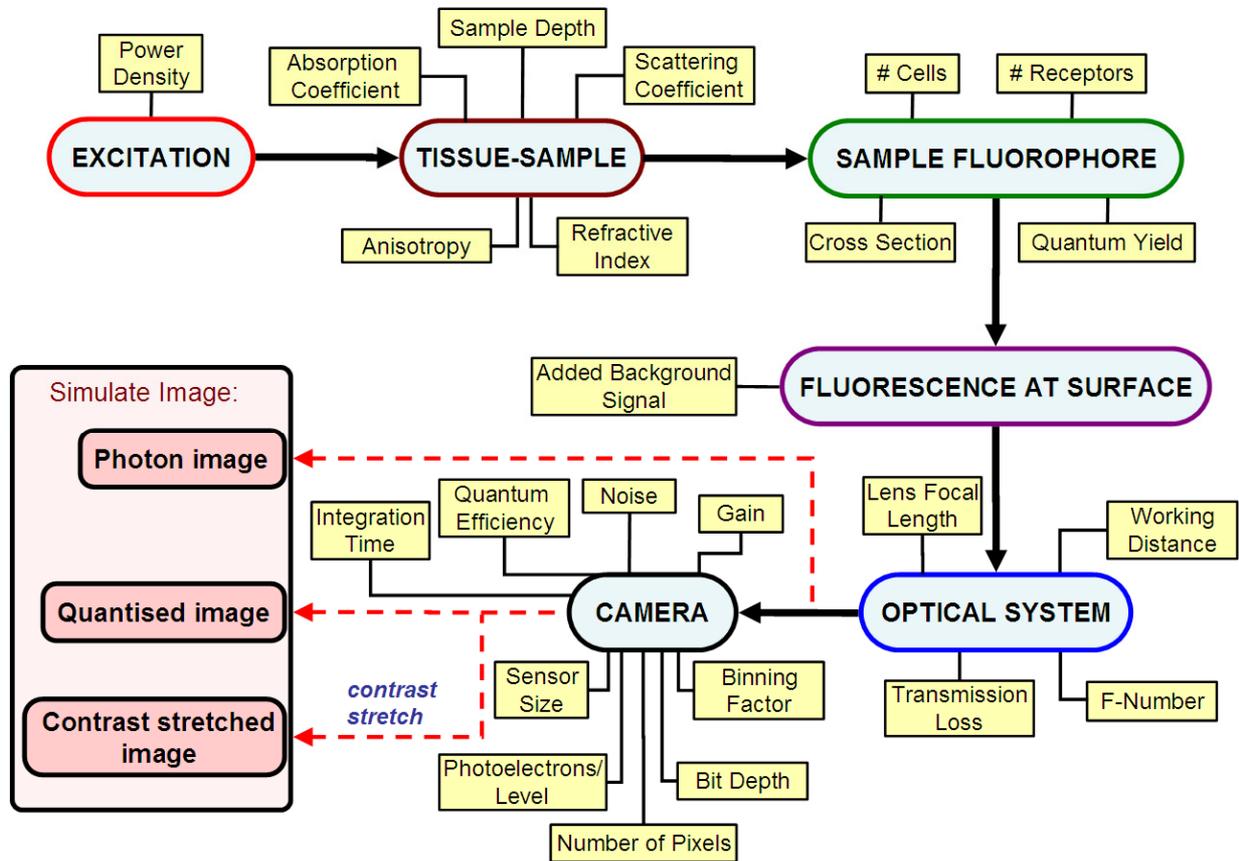

Figure 5: FIFAC flowchart. The user can set the parameters included in the yellow boxes. The output of the software consists of three different simulated images (red box) that are individually displayed.

The parameters inside the edit boxes, the sliders and the radio buttons are user-set (see also yellow boxes in the flowchart). All the other parameters are updated when the simulation is performed. This happens when any of the "Simulate Image" buttons are pressed. Default parameters are already assigned when we start the software.

The size of the fluorescent sample is determined by the imaged pixel dimension: a maximum cell number is allowed to be present in the sample volume: we assume a cell diameter of 10 μm in this simulation. However, as we place the sample deeper into the tissue, larger sample volumes would still behave as point sources, allowing a higher number of cells to 'fit' in the sample volume. We have implemented this by considering the size of the sample to be equivalent to the size of the pixel +10% of the extent of the photon distribution on the surface. A warning message pops up when the number of cells selected is unlikely to fit in the sample.

The user is free to change tissue parameters. However, when the values are far from what is typical in biological tissues (e.g. when $\mu_A > \mu_S$), the analytical solution based on the diffusion approximation does not guarantee a good agreement with the Monte Carlo method. If that happens, FIFAC will warn the user that something might be wrong with the estimation of the photon flux.
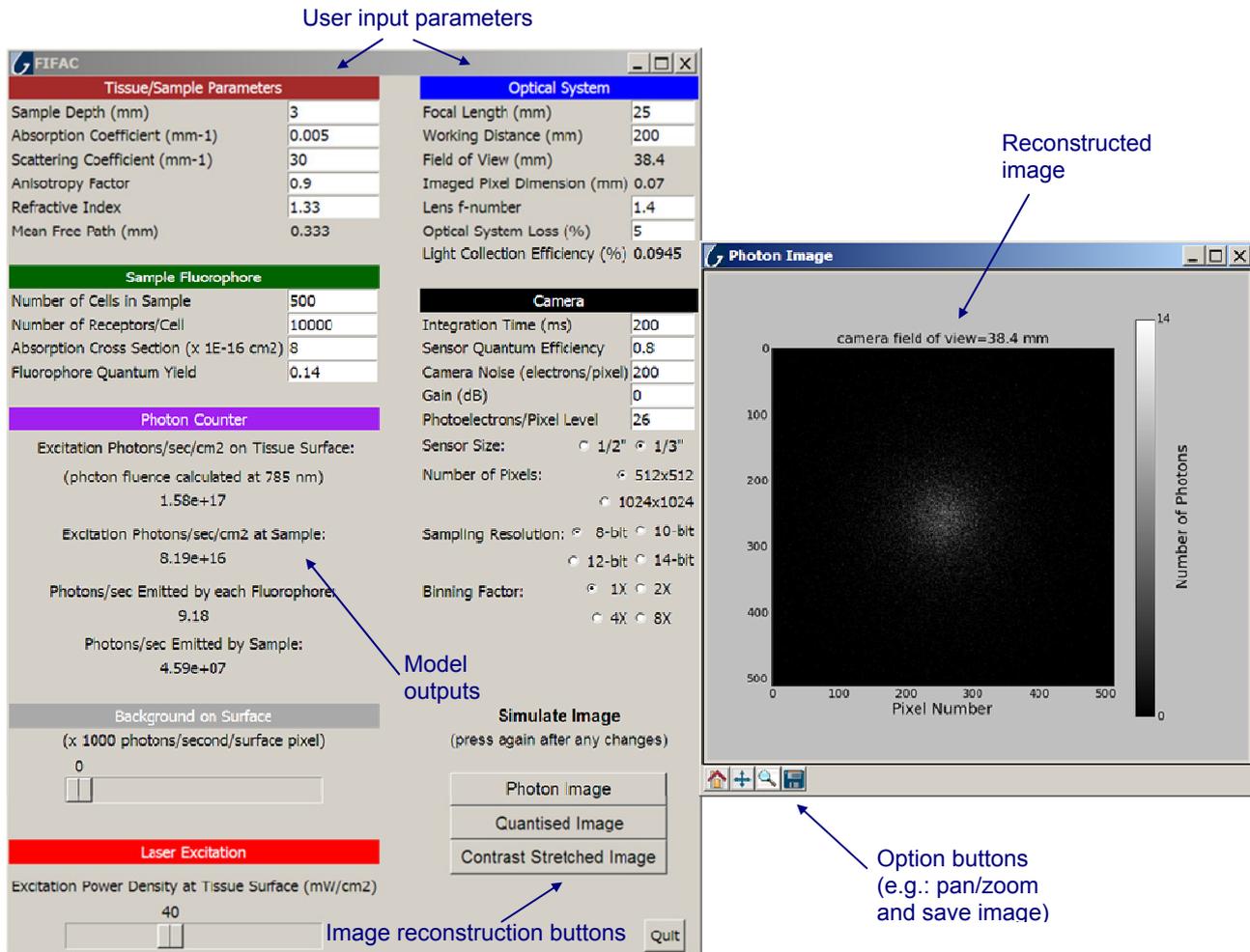
Figure 6: FIFAC graphical interface. The left window contains the input parameters and the output numerical values. The right window pops up after clicking the button corresponding to the desire image reconstruction. The figure can be updated with new parameters by pressing the same button. A toolbar at the bottom allows the user to zoom in/out, select region of interests, move within the plot and save the figure.

8. Image reconstruction

We developed a software interface that allows direct visualization of the imaged surface. Using an approximated solution of the diffusion equation [5], we estimate the photon fluence first on the surface of the tissue and then on the imaging sensor. What we obtain is a map (shown in Figure 7(a)) that represents the amount of light collected by the imager. Due to the statistical nature of the photon detection process, the amount of light is given by generating random numbers from the Poisson distribution with mean parameter the average number of photons expected. The quantised image that would appear on a screen was achieved by setting appropriate values for the sensor quantum efficiency and the photoelectrons/pixel level conversion factor. The software default value was set to 26, a value which corresponds to one of the more sensitive non-cooled CCD imagers; this was determined experimentally for a Sony XC-505P camera. Figure 7(b) shows the image after analogue-to-digital conversion. The bit depth and binning factor can be selected by the user (the default value is 8-bit and 1x binning). Binning improves the signal-to-noise ratio at the expense of spatial resolution, by adding intensity values from adjacent pixels.

Prior to reconstruction, the user can set the average background level in terms of photons/surface pixel, which, in practical situation, can be caused by external light sources, tissue autofluorescence or excitation light not fully rejected by the imaging system's emission filter. The detection noise

(typical of every imaging sensor), as well as gain and integration time, can also be set by the user, making the software effective in simulating the complete imaging system's performance.
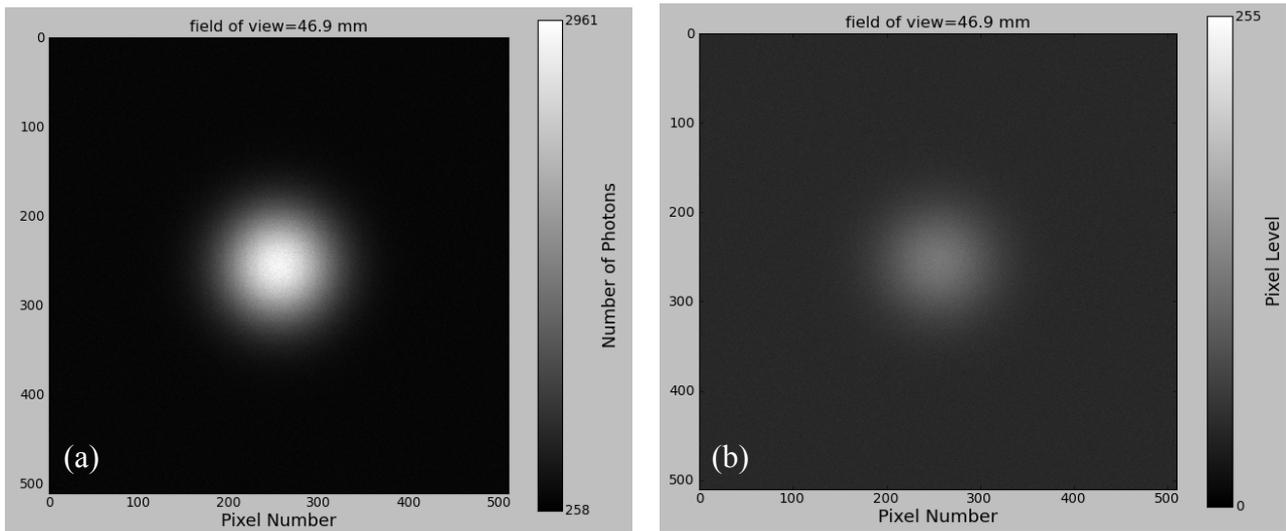

Figure 7: (a) Monochrome map of the photons collected by the sensor. (b) Same image following digitisation. The images are the result of fluorescence emission from a sample located at 5 mm depth. Note that (a) is automatically scaled to the range of values, whereas (b) always maintains the 256 levels typical of an 8-bit converter

9. Image processing

During fluorescence imaging, the signal-to-background ratio can be low, particularly when a dye is imaged at high depth and/or additional light sources are present. In these situations, the fluorescence signal can be difficult to detect, due to the low contrast between adjacent pixel levels. However, if the whole range of levels is used to express the intensities between the minimum and the maximum pixel level of the image, the apparent contrast can be increased and any potential image rendered visible. By pressing the button "Contrast Stretched Image" the user can increase the contrast of the image as described above. The final result becomes effective particularly when the fluorescence signal is not clearly visible (Figure 8). The values at the extremities of the greyscale intensity bar indicate the lowest and the highest pixel amplitude levels of the image.
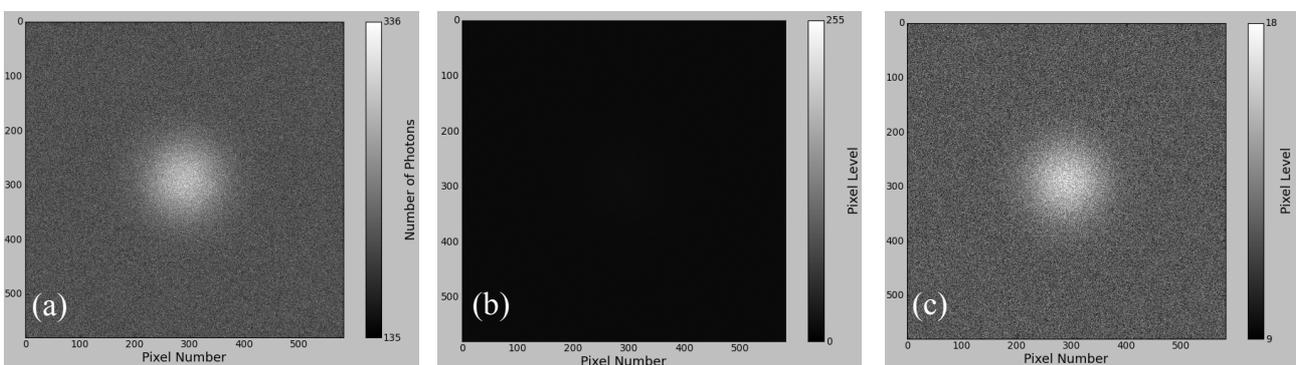

Figure 8: Same image expressed in number of photons collected (a) and pixel intensity (b). With a conversion factor of ~26 photoelectrons/pixel, only ~9 intensity levels separate the central peak from the background. As a consequence, the signal is difficult to see in (b). Figure (c) represents the result of the 'contrast stretch' function applied to the same image, which uses the whole range of display intensities to represent the intensity levels between the higher (in this case 18) and the lower (9) pixel level.

10. Conclusions

The software we developed provides a fast and effective way to estimate light flux in a 'deep' tissue fluorescence imaging system. The model can easily be adapted to other simple geometrical configurations and to reflectance imaging. The Monte Carlo method still remains the best approach to follow when the complexity of the system is higher (such as when the tissue is not homogeneous). However, when a low level of precision is required, an analytical model can provide fast and convenient solutions.

References

[1] Lihong V. Wang, Hsin-i Wu: Biomedical Optics - Principles and Imaging, Wiley-Interscience, 2007.

[2] Prahl, S.A., M. Keijzer, S.L. Jacques, A.J. Welch: A Monte Carlo model of light propagation in tissue. In Dosimetry of Laser Radiation in Medicine and Biology, G. Mueller, D. Sliney, Eds., SPIE Series Vol. IS 5:102-111, 1989.

[3] Cheong, W. F., Prahl, S. A., Welch, A. J.: A Review of the Optical Properties of Biological Tissues, IEEE Journal of Quantum Electronics, vol. 26, issue 12, pp. 2166-2185, 1990.

[4] Xu C., Williams R. M., Zipfel W. and Webb W. W.: Multiphoton excitation cross-sections of molecular fluorophores, Bioimaging 4, 198–207, 1996.

[5] Farrell, T.F., Patterson, M.S. (2003) Diffusion modeling of fluorescence in tissue. In: Mycek, M.A., Pogue, B.W. Handbook of biomedical fluorescence. Marcell Dekker, New York, pp 29–60